

Received 21 June 2024, accepted 1 July 2024, date of publication 8 July 2024, date of current version 18 July 2024.

Digital Object Identifier 10.1109/ACCESS.2024.3425159

RESEARCH ARTICLE

Dual Functional Liquid Displacement and Angular Detection Based on Band Stop Response Microwave Sensor

SYAH ALAM¹, (Graduate Student Member, IEEE), INDRA SURJATI¹, (Member, IEEE), LYDIA SARI¹, (Member, IEEE), R. DEINY MARDIAN¹, (Member, IEEE), MAROUANE ABICHA², (Student Member, IEEE), ZAHRIADHA ZAKARIA³, (Senior Member, IEEE), TEGUH FIRMANSYAH⁴, (Member, IEEE), MUDRIK ALAYDRUS⁵, (Senior Member, IEEE), AND YUSNITA RAHAYU⁶, (Senior Member, IEEE)

¹Department of Electrical Engineering, Universitas Trisakti, West Jakarta 11440, Indonesia

²Department of Electrical Engineering, Polytechnic Nantes, 44300 Nantes, France

³Faculty of Electronic and Computer Technology and Engineering, Universiti Teknikal Malaysia Melaka (UTeM), Durian Tunggal 76100, Malaysia

⁴Department of Electrical Engineering, Universitas Sultan Ageng Tirtayasa, Serang, Banten 42124, Indonesia

⁵Department of Electrical Engineering, Universitas Mercu Buana, West Jakarta 11650, Indonesia

⁶Department of Electrical Engineering, Universitas Riau, Pekanbaru 28292, Indonesia

Corresponding authors: Syah Alam (syah.alam@trisakti.ac.id) and Zahriladha Zakaria (zahriladha@utem.edu.my)

This work was supported by Ministry of Education and Culture, Republic of Indonesia, Institute for Research and Community Service Universitas Trisakti. The author extends their appreciation to Universiti Teknikal Malaysia Melaka (UTeM) to support the study under grant Jurnal/2022/FTKEK/Q00086.

ABSTRACT This paper proposes dual functional microwave sensor for displacement and angular detection of liquid material based on electric coupled (ELC) resonator. The proposed resonator uses a two-port band stop filter operating at a resonant frequency of 2.72 GHz. Polystyrene-mm pipe channels are used to accommodate water samples placed in the sensing area of the sensor in the center of the ELC resonator. Displacement and angular detection were observed based on the shift in the resonant frequency of the resonator. Based on the measurement results, the proposed sensor has a sensitivity for displacement detection of 31.5 MHz/cm with a distance range of $d = 1 - 4$ cm while for angular detection it is 0.33 MHz/ $^{\circ}$ with a rotation angle of $0 - 90^{\circ}$ for polystyrene-mm pipe channel filled with water content. This paper makes a significant contribution by proposed a dual functional microwave sensor for displacement and angular detection that can be recommended for the automotive, robotics and aerospace industries.

INDEX TERMS Dual functional, displacement, angular, polystyrene-mm pipe, microwave sensor.

I. INTRODUCTION

Displacement sensors play an important role for several industries that require high precision such as the automotive, robotics and aerospace industries [1], [2], [3], [4]. Generally, displacement sensors consist of two types, including linear and angular displacement. Linear displacement is determined based on distance while angular displacement is based on the angle between the sensor and the sample [5], [6]. One of the strategies for detecting sample displacement is to utilize

The associate editor coordinating the review of this manuscript and approving it for publication was Li Yang¹.

a microwave sensor [7], [8], [9], [10]. Microwave sensors have advantages including compact design, low cost and high accuracy. Microwave sensors have been widely developed to detect the characteristics of solid materials [11], [12], [13], liquids [14], [15], [16], [17] and displacement [18], [19], [20]. Several previous works proposed sensors for linear and angular displacement detection in solid materials using microwave sensors with a certain dynamic range based on frequency shift [21], [22], notch depth [23], [24] and phase variation [25], [26]. Generally, rotation and displacement detection using microwave sensors is proposed for solid materials using stators and rotators where the sample is rotated in the

sensing area with a certain dynamic range [27], [28], [29]. However, this creates friction between the sample and the sensor which has the potential to damage the surface of the sensor. In addition, the sample is placed on an open surface, so it is greatly influenced by changes in temperature and environment. Another constraint, the proposed sensor from previous work only has one single function so it cannot be used for displacement and rotation detection separately. In addition, sensors for displacement and rotation detection are only proposed for solid materials and are not supported for detection in liquid samples. Therefore, microwave sensors that have the capability to detect displacement and rotation of liquid samples are needed. Moreover, liquid displacement sensors are very useful for several applications, including biomedical and robotics [30], health monitoring and mobile healthcare [31]. This work provides an excellent solution by proposing a microwave sensor that has dual functional characteristics for displacement and angular detection for liquid samples. Furthermore, to maintain and control the influence of temperature and environment, the sample is contained in a polystyrene-mm pipe channel [32], [33], [34]. Moreover, polystyrene-mm pipe is proposed to reduce friction between the sensor and the sample so that the sensor surface is more durable and protected. Displacement and angular detection are determined based on the shift in the resonant frequency of the resonator. The main contribution of this work is to produce a dual functional microwave sensor that has the capability for displacement and angular detection in liquid samples in polystyrene-mm pipe channels. The proposed sensor has been successfully simulated and validated through the measurement process. Based on the measurement results, the proposed sensor has the ability to detect liquid displacement with a distance range of 1 - 4 cm and for angular detection with an angle range of 0 - 90°.

II. WORKING PRINCIPLE OF PROPOSED SENSOR

This section explains in detail the development model, structure of the ELC resonator and the sample placement scenario of the proposed sensor.

A. STRUCTURE OF ELC RESONATOR

The proposed microwave sensor based on ELC resonator uses RO4003C with permittivity of 3.55, tan δ of 0.0027 and thickness of 0.587 mm. The proposed resonator operates at a resonant frequency of $f_r = 2.69$ GHz with two ports representing P1 and P2. The structure of the proposed sensor is shown in Fig. 1(a) while the concentration of the electric field and magnetic field is shown in Fig. 1(b) and Fig 1(c). The structure of the ELC resonator consists of the left and right inductive arms, while the capacitive area is in the gap between the strips in the middle of the resonator. The overall dimension of ELC resonator is shown in Table 1. Based on the simulation results using HFSS 15.0, the highest electric field concentration at $f_r = 2.69$ GHz is in the arms and gaps between the strips of the ELC resonator as shown in Fig.1 (b),

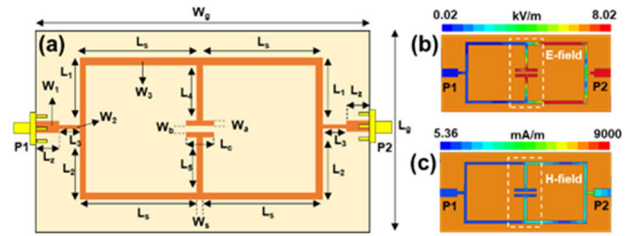


FIGURE 1. (a) Structure of electric field coupled resonator, (b) E-field at $f_r = 2.69$ GHz, (c) H-field at $f_r = 2.69$ GHz.

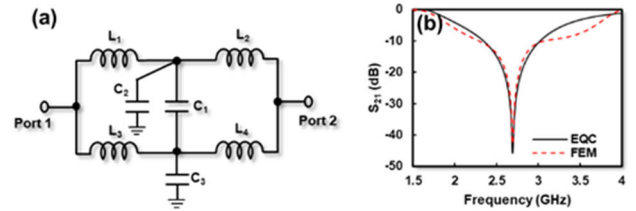


FIGURE 2. (a) Equivalent circuit of electric field coupled resonator, (b) comparison of EQC and FEM of electric field coupled resonator.

TABLE 1. Dimension of proposed ELC resonator.

| Parameter | Value (mm) | Parameter | Value (mm) |
|-----------|------------|------------|------------|
| W_g | 70 | L_4 | 9 |
| L_g | 30 | L_5 | 9 |
| L_s | 24.5 | L_c | 9 |
| L_1 | 11 | L_z | 7 |
| L_2 | 11 | W_a | 1 |
| L_3 | 3 | W_b | 1 |
| W_1 | 3 | W_2, W_3 | 1 |

while the magnetic field concentration vanishes as shown in Fig.1 (c).

Based on perturbation theory, the area of the resonator with a high electric field can be used to detect the characteristics of the sample [35].

Furthermore, the equivalent circuit of the ELC resonator can be derived based on L and C model as shown in Fig.2 (a). The arm of the resonator is represented as an inductor while the gap between strip is represented as a capacitor. The values of L and C are extracted using AWR 2009 where $L_1 = L_2 = L_3 = L_4 = 8.23$ nH, $C_1 = 0.17$ pF and $C_2 = 0.99$ pF and $C_3 = 1.25$ pF which are connected to port 1 and port 2 with an impedance of 50 Ω. Therefore, the resonant frequency (f_r) of resonator can be determined using following Eq. (1) [36]:

$$f_r = \frac{1}{2\pi\sqrt{LC}} \tag{1}$$

A comparison of the simulation results from EQC and FEM is shown in Fig. 2 (b) where the results are both in line and operating at $f_r = 2.69$ GHz.

B. DEVELOPMENT MODEL OF ELC RESONATOR

The ELC resonator was developed in two steps where the proposed characteristic is a band stop response. The model

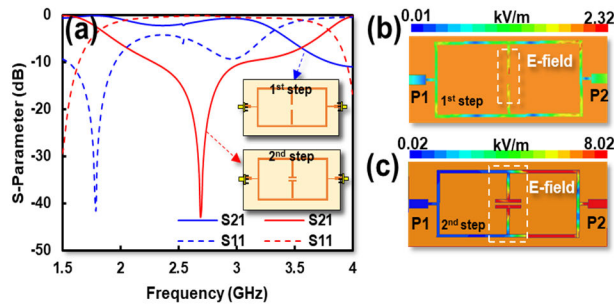


FIGURE 3. Development model of ELC resonator; (a) response of S-parameters, (b) E-field concentrations of ELC resonator at 1st and 2nd step.

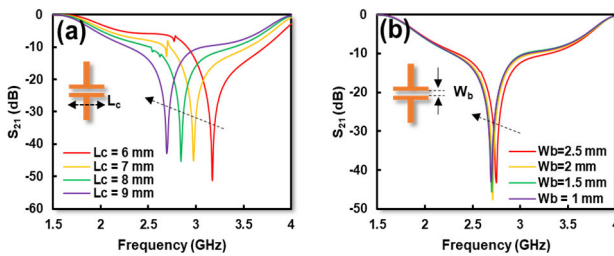


FIGURE 4. Iteration process; (a) iteration of L_c , (b) iteration of W_b .

development of the ELC resonator is shown in **Fig. 3 (a)**, **Fig. 3 (b)** and **Fig. 3 (c)**.

The characteristics of the S-parameters at the 1st step show that the resonator has a band pass response where $S_{11} \leq -10$ dB while $S_{21} \geq -10$ dB in the frequency range of 1.5 - 3.2 GHz as shown by the red line in **Fig. 3 (a)**. Furthermore, for the 2nd step, the characteristics of the S-parameters show the band stop response where $S_{11} \geq -10$ dB while $S_{21} \leq -10$ dB in the frequency range of 1.7 GHz - 3.82 GHz as shown by the blue line in **Fig. 3 (a)**. In addition, the characteristics of the electric field of the resonator for the 1st and 2nd steps are also observed as shown in **Fig. 3 (b)** and **Fig. 3 (c)**. The electric field concentration is observed at $f_r = 2.69$ GHz where for the 1st step the electric field is concentrated in the center of the ELC resonator while for the 2nd step it is in the gap between the strips of the ELC resonator.

Next, several iterations are carried out to control the resonant frequency and S_{21} of the resonator as shown in **Fig. 4 (a)** and **Fig. 4 (b)**. **Fig. 4 (a)** shows that the iteration of L_c causes the resonance frequency to shift lower in line with increasing length of L_c . In addition, the gap between the strips of the ELC resonator represented by W_b also has an impact on the resonant frequency and S_{21} of the resonator. Increasing the gap width W_b causes the resonant frequency of the resonator to shift towards high. This finding shows that the gap in the strip is an area that has high sensitivity so it can be recommended as a sensing area for placing samples.

C. FABRICATION OF PROPOSED RESONATOR

The fabrication results of the front and back side of the resonator are shown in **Fig. 5 (a)** and **Fig. 5 (b)** where the ELC resonator is in the front layer and the ground plane is in the back layer. The ELC resonator is connected to port 1 and

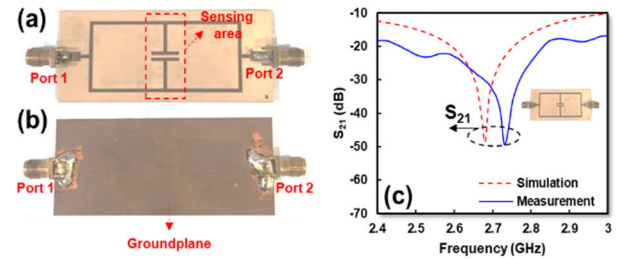


FIGURE 5. (a) Fabrication of ELC resonator at the front side, (b) fabrication of ELC resonator at the back side, (c) simulation and measurement of proposed resonator.

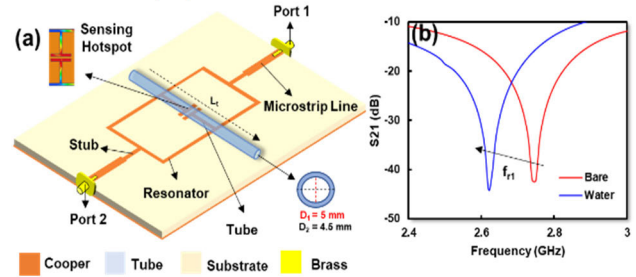


FIGURE 6. (a) Scenario placement of sample, (b) simulation of bare and with water condition.

port 2 and has the characteristics of a Band Stop Filter (BSF). Moreover, the comparison of simulation and measurement results from the resonator is shown in **Fig. 5 (c)**.

Based on the measurement results, there is a slight difference between measurement and simulation result where the resonance frequency shifts from 2.69 GHz to 2.72 GHz. This is due to errors from the fabrication process and the permittivity of RO4003C which is in the range 3.38 - 3.55 [37], [38].

D. SCENARIO OF SAMPLE PLACEMENT

The sample placement scenario is determined based on the location of the resonator with the highest electric field as shown in **Fig. 6 (a)**. In this paper, the sample is placed in the center of the ELC resonator using a polystyrene-mm pipe channel based on polystyrene-mm pipe channel [17] with a permittivity of 3.1 and a diameter represented by D_1 and D_2 of 5 mm and 4.5 mm and length of polystyrene-mm pipe channel represented by L_t of 40 mm, respectively. The sample placement scenario consists of two conditions, including the bare condition where the polystyrene-mm pipe channel is filled with air samples and the other condition is when the polystyrene-mm pipe channel is filled with water samples. The polystyrene-mm pipe channel is placed in line with the sensing area of the ELC resonator which is located in the middle arm and the gap of the resonator.

The simulation results from bare conditions and with water samples shown in **Fig. 6 (b)** show that the resonance frequency of the resonator moves to the lower frequency from 2.75 GHz to 2.62 GHz because the permittivity of water is higher than bare where the permittivity of water is $\epsilon_r = 80$ and bare is $\epsilon_r = 1$. Furthermore, to demonstrate the performance

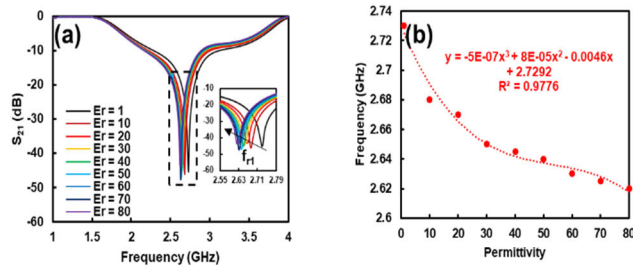


FIGURE 7. (a) Simulation with range ϵ_r of 1 – 80, (b) correlation between frequency and permittivity range ϵ_r of 1 – 80.

of the proposed sensor, the permittivity of the sample inside the polystyrene-mm pipe channel is changed to a permittivity range of $\epsilon_r = 1 - 80$. Based on Fig.7 (a), the resonant frequency of the resonator shifts from 2.73 GHz to 2.62 GHz with a permittivity range of 1 – 80 with ΔF of 0.11 GHz.

It should be noted, based on the simulation results from Fig. 7 (a) and Fig.7 (b), it shows that changes in the permittivity of the sample in the polystyrene-mm pipe channel greatly affect the resonant frequency of the resonator where the resonant frequency moves to a lower frequency in line with an increase in the permittivity of the sample.

III. MEASUREMENT RESULT AND VERIFICATION

In this chapter, the measurement process and scenarios for liquid displacement and angular detection are explained in detail. The measurement process was carried out in the laboratory using a Vector Network Analyzer (VNA) with a frequency range of 2 - 3 GHz, a frequency step size of 0.01 GHz and an ambient temperature of 25° C.

A. SCENARIO FOR LIQUID DISPLACEMENT DETECTION

The proposed resonator consisting of port 1 and port 2 is connected to the vector analyzer using a coaxial cable with an impedance of 50Ω where the sensor and sample are placed using a holder as shown in Fig 8(a) . Liquid displacement detection is proposed by placing a stopper in the center of the sample in a polystyrene-mm pipe channel filled with water content as shown in Fig. 8 (b).

It should be noted, the sample in the plastic tube [17] placed carefully and is in direct contact with the sensing area in the middle of the ELC resonator. The stopper is placed in the middle of the polystyrene-mm pipe channel so that the water sample inside is clogged. Additionally, the area of the clogged polystyrene-mm pipe channel is filled with air samples represented by bare. The sample in the polystyrene-mm pipe channel will be moved vertically using a holder with a distance d of 1 - 4 cm as shown in Fig.8 (c). Furthermore, liquid displacement detection is determined by observing the shift in the resonance frequency when the sample moves through the sensing area of the resonator.

Based on the measurement results, the resonant frequency of the resonator shifts from 2.716 GHz to 2.59 GHz with ΔF of 0.126 GHz in line with the sample displacement in the polystyrene-mm pipe channel which is clogged by a stopper

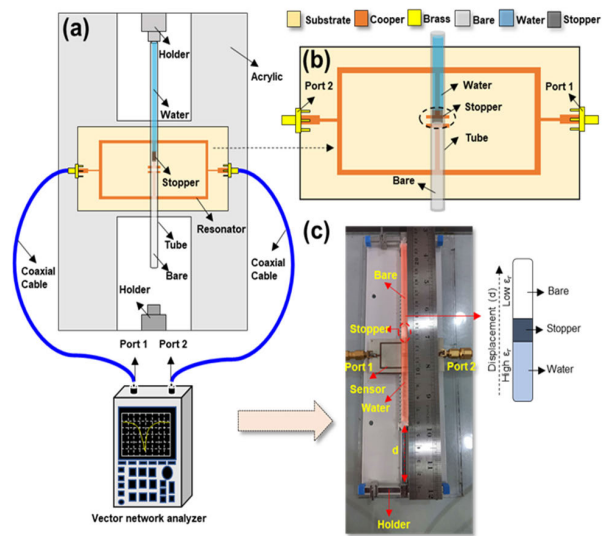


FIGURE 8. (a) Scenario for liquid displacement detection, (b) detail structure of liquid displacement detection, (c) measurement setup for liquid displacement detection using proposed sensor.

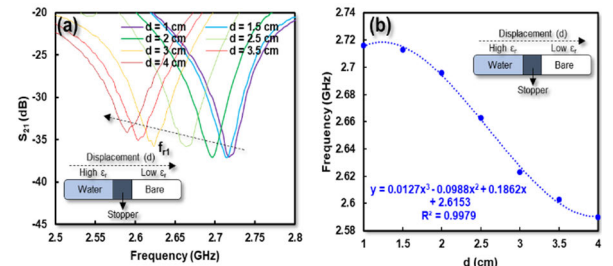


FIGURE 9. (a) Measurement result of liquid displacement detection with $d = 1 - 4$ cm, (b) correlation between resonant frequency and liquid displacement with $d = 1 - 4$ cm.

with a distance range of $d = 1 - 4$ cm as shown in Fig.8 (a) and Fig.8 (b). This finding shows that the proposed sensor has interacted with the sample to detect the displacement of the sample. The resonant frequency of the resonator shifts to low frequencies slowly in line with the displacement of the sample. This occurs because there is a change in the permittivity of the sample, where the water sample has a higher permittivity than the bare air sample, so it greatly influences the resonance frequency of the resonator. Furthermore, displacement detection with the proposed resonator can be determined based on Eq. (2) [7]:

$$f_{r(c)} = 0.01273 d^3 - 0.988 d^2 - 0.1862 d - 2.6153 \quad (2)$$

where $f_{r(b)}$ is the resonant frequency of the resonator for displacement detection and d represents the distance of the displacement in the water-filled polystyrene-mm pipe channel.

Moreover, the sensitivity (S) of the sensor is determined based on the following Eq. (3) [21]:

$$S = \frac{\Delta F \text{ (GHz)}}{\Delta d \text{ (cm)}} \quad (3)$$

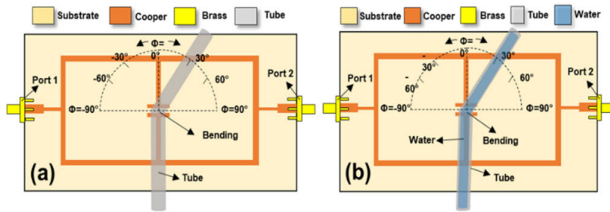


FIGURE 10. Scenario of angular detection from 0° - 90°; (a) without water, (b) with water.

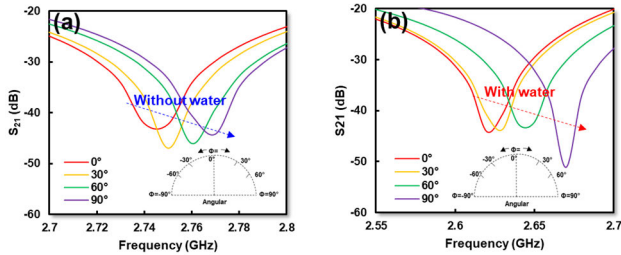


FIGURE 11. Simulation result of angular detection from 0° - 90°; (a) without water, (b) with water.

where ΔF represents the shift in the resonant frequency of the resonator and Δd represents the displacement of the sample in the polystyrene-mm pipe channel. Based on Eq. (3), the sensitivity of the sensor for displacement detection is 31.5 MHz/cm with a range d of 1 - 4 cm.

B. SCENARIO FOR LIQUID ANGULAR DETECTION

Furthermore, liquid angular detection is proposed by rotating the sample inside the polystyrene-mm pipe channel with an angle range of 0° - 90°. In this paper, the rotation of the sample in the polystyrene-mm pipe channel is divided into two conditions, including with water and without water as shown in Fig. 10 (a) and Fig.10 (b). The sample in the polystyrene-mm pipe channel is rotated clockwise at angles of 0°, 30°, 60° and 90°.

The simulation results in Fig.11 (a) and Fig.11 (b) show that the resonant frequency of the resonator shifts to a higher frequency in line with increasing the rotation angle of the sample for conditions without water and with water content. The resonant frequency shifts from 2.74 GHz to 2.77 GHz in conditions without water, while for conditions with water it shifts from 2.62 GHz to 2.67 GHz with an angle range of 0° - 90° as shown in Fig. 12 (a) and Fig. 12 (b).

Furthermore, validation of angular detection is carried out by measuring the process using a VNA connected to port 1 and port 2 of the resonator placed in the holder using a coaxial cable with an impedance of 50 Ω. The sample in the polystyrene-mm pipe channel is carefully placed in the sensing area which is located in the middle of the ELC resonator as shown in Fig.13 (a) and Fig.13 (b).

Moreover, to ensure that the sample position is constant and stable, a gripper is proposed in the measurement setup to lock the position of the sample and sensor. The measurement results of angular detection when the polystyrene-mm pipe channel is filled with water and without water are shown in Fig.14 (a) and Fig.14 (b).

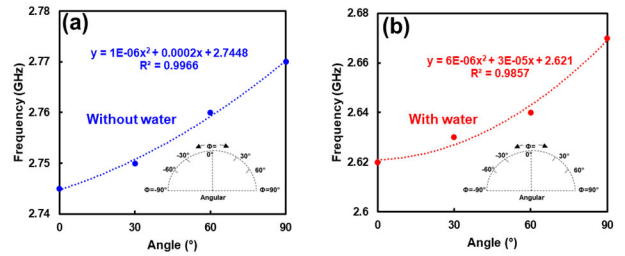


FIGURE 12. Simulation result of correlation between resonant frequency and angle from 0° - 90°; (a) without water, (b) with water.

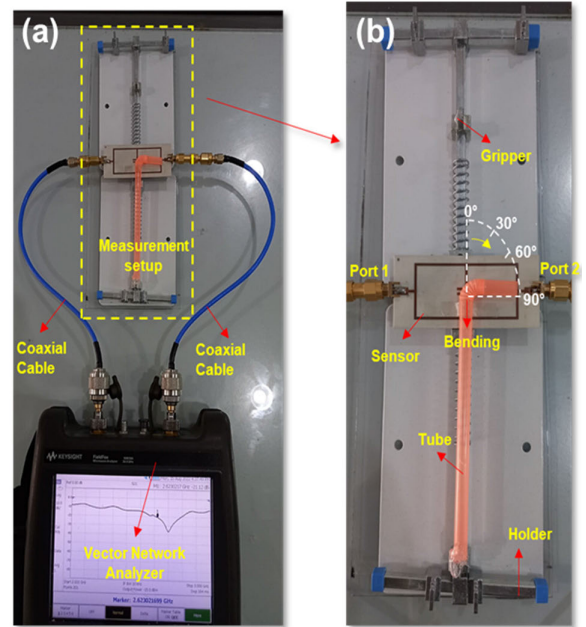


FIGURE 13. (a) Measurement setup with VNA, (b) Measurement scenario for angular detection from 0° - 90°.

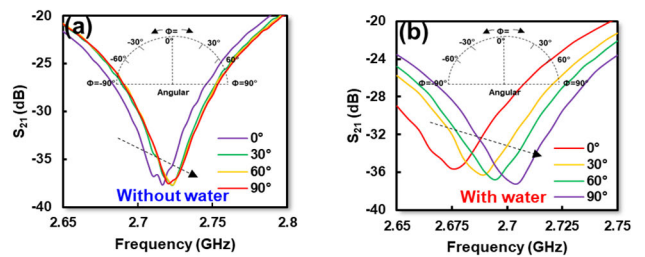


FIGURE 14. Measurement result of angular detection from 0° - 90°; (a) without water, (b) with water.

Based on the measurement results, the frequency of the resonator shifts from 2.716 GHz to 2.723 GHz when the polystyrene-mm pipe channel is without water, whereas when the polystyrene-mm pipe channel is filled with water, the frequency shifts from 2.675 GHz to 2.705 GHz with an angle range of 0° - 90° as shown in Fig.15 (a) and Fig.15 (b). These findings indicate that the proposed sensor interacts with the sample so that the resonant frequency of the resonator changes in line with an increase in the rotation angle of the sample in the polystyrene-mm pipe channel.

It should be noted, the resonance frequency shifts to a higher frequency due to the interaction of the sample and

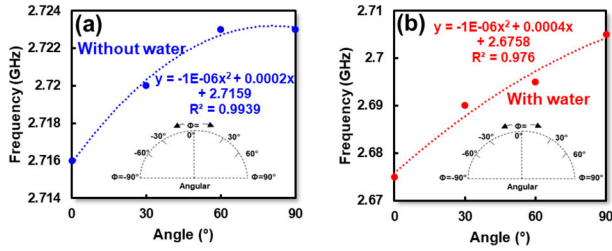


FIGURE 15. Measurement result of correlation between resonant frequency and angular from 0° - 90°; (a) without water, (b) with water.

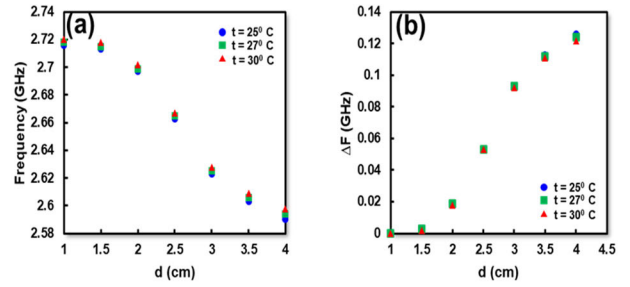


FIGURE 17. Displacement detection of liquid samples based on different temperatures; (a) response of the resonant frequency, (b) ΔF of proposed sensor.

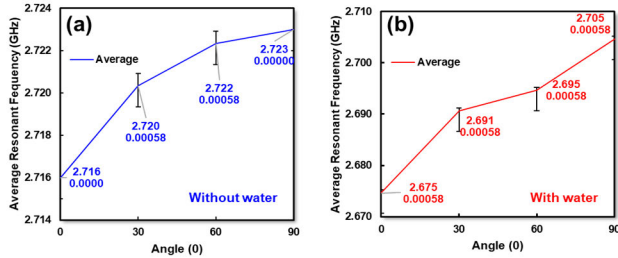


FIGURE 16. Average and deviation from repeatability measurement for angular detection; (a) without water, (b) with water.

sensor which changes while the sample inside polystyrene-mm pipe channel shifts away from the surface of the sensing area with water content to bare condition (without sample). In other words, the permittivity of the sample changes from higher to lower. This condition changes the concentration of the electric field of the resonator and greatly influences the resonant frequency of the resonator.

Furthermore, angular detection of polystyrene-mm pipe channel without and with water can be determined based on the following Eq. (4) and Eq. (5):

$$f_r (ba) = -0.000001 x^2 - 0.0002 x + 2.7159 \quad (4)$$

$$f_r (bw) = -0.000001 x^2 - 0.0004 x + 2.6578 \quad (5)$$

where $f_r (ba)$ and $f_r (bw)$ is the resonant frequency of the resonator for angular detection with and without water and x represents the angle of the angular in the water-filled polystyrene-mm pipe channel.

Moreover, the sensitivity (S) of the sensor is determined based on the following Eq. (6) [18]:

$$S = \frac{\Delta F \text{ (GHz)}}{\Delta \theta \text{ (°)}} \quad (6)$$

where ΔF represents the shift in the resonant frequency of the resonator and $\Delta \theta$ represents the rotation of the sample in the polystyrene-mm pipe channel.

Based on Eq. (6), the sensitivity of the sensor for angular detection of polystyrene-mm pipe channel without and with water content are 0.07 MHz/° and 0.33 MHz/° with a dynamic range of 0 - 90°. Moreover, average and deviation of repeatability measurements with 3 cycles are proposed to show the error bars of angular detection for sample filled in polystyrene-mm pipe channel with and without water using the proposed sensor as shown in Fig.16.

Based on Fig.16 (a) and Fig. 16 (b), the deviation from the repeatability measurement results is in the range 0 - 0.00058 for angular detection with and without water. These findings indicate that the proposed sensor has a low error bar for angular detection in samples with and without water. To show the effect of changing the temperature of the liquid sample on displacement detection, validation with measurements at three different temperatures is proposed as shown in Fig. 17 (a) and Fig. 17 (b).

Referring to Fig.17 (a), changes in temperature in the sample have an impact on shifting the resonant frequency of the resonator towards high frequencies correlated with previous work [34] [39]. The maximum ΔF of the proposed sensor for three different temperatures are 0.126 GHz, 0.124 GHz and 0.122 GHz respectively as shown in Fig. 17 (b). The sensitivity of the sensor based on temperature changes is 31.5 MHz/cm, 31 MHz/cm and 30.5 MHz/cm respectively. These findings indicate that changing the temperature of the sample has an impact on the shift in the resonance frequency and sensitivity of the sensor but is not significant. Therefore, the temperature of the sample must be verified before the measurement process is carried out to obtain optimal performance.

IV. VALIDATION WITH PREVIOUS WORK

To validate the performance of the proposed sensor, a comprehensive evaluation with previous work is proposed as shown in Table 2. Based on previous work, the detection of linear and angular displacement of samples using microwave sensors are divided into three types of mechanisms based on frequency shift, phase variation and notch depth.

Previous work [1], [32] proposed a microwave sensor based on transmission line for displacement detection of solid materials with a maximum dynamic range of 3 - 40 mm and maximum sensitivity of 312.7 ° / mm and 528.7 ° / mm where the displacement detection was determined based on phase variations. However, the sensor only has one function for displacement detection and cannot be used for angular displacement of materials. Other works [7], [23] proposed a microwave sensor for displacement and rotation detection of solid materials based on notch depth with a maximum dynamic range of 10 mm and 90 °. Nevertheless, the proposed sensor only supports displacement detection in solid

TABLE 2. Comparison of proposed sensor based on displacement / rotation technique with existing works.

| Ref | Method | Freq (GHz) | Sensing mechanism | Sample | Dynamic Range | | Sensitivity Average | | Polystyrene mm-pipe | Sensor Type | | Dual Functional |
|------------------|--------------------------------------|-------------|-------------------|---------------|-----------------|----------------|---------------------|-------------------|---------------------|--------------|------------|-----------------|
| | | | | | Displacement | Angular | Displacement | Angular | | Displacement | Angular | |
| [1] | Step impedance transmission lines | 2.00 | Phase variation | Solid | 0 – 40 mm | - | 312.77°/mm | - | - | Yes | - | - |
| [3] | H-shaped resonator | 4.80 | Freq shift | Solid | 0 – 12 mm | - | 147.8 MHz/mm | - | - | Yes | - | - |
| [7] | Dielectric resonator | 3.70 | Notch depth | Solid | 1 – 10 mm | - | 0.095 dB/mm | - | - | Yes | - | - |
| [19] | Transversal signal interference | 0.92 | Freq shift | Solid | - | 0 – 180° | - | 3.15 MHz/° | - | - | Yes | - |
| [21] | CSRR | 5.80 | Freq shift | Solid | - | 0 – 90° | - | 2.37 MHz/° | - | - | Yes | - |
| [23] | Transmission line | 1.21 | Notch depth | Solid | - | 0 – 90° | - | 0.095 dB/° | - | - | Yes | - |
| [27] | TFS - coupled slot line | 2.17 | Freq shift | Solid | - | 0 – 90° | - | 2.27 MHz/° | - | - | Yes | - |
| [28] | U-shaped resonator | 1.20 | Freq shift | Solid | - | 0 – 180° | - | 1.94 MHz/° | - | - | Yes | - |
| [32] | Stepped impedance Transmission lines | 2.00 | Phase variation | Solid | 0 – 3 mm | - | 528.7°/mm | - | - | Yes | - | - |
| This work | ELC Resonator | 2.72 | Freq shift | Liquid | 1 – 4 cm | 0 – 90° | 31.5 MHz/cm | 0.33 MHz/° | Yes | Yes | Yes | Yes |

TABLE 3. Comparison of type, sensing parameters and prospective applications of displacement / rotation sensors.

| Ref | Type of resonator | Sensing parameter | Prospective applications |
|------------------|-------------------------|-----------------------|----------------------------------|
| [1] | Single port resonator | Phase | Industrial |
| [3] | Band stop filter | S ₂₁ | Industrial |
| [7] | Band pass filter | S ₂₁ | Industrial |
| [19] | Band stop filter | S ₂₁ | Industrial |
| [21] | Band stop filter | S ₂₁ | Space vehicle (satellites) |
| [23] | Band pass filter | Phase | Industrial |
| [27] | Band pass filter | S ₂₁ | Industrial |
| [28] | Band stop filter | S ₂₁ | Industrial |
| [32] | Band pass filter | S ₂₁ | Biomedical and energy |
| This work | Band stop filter | S₂₁ | Industrial and Biomedical |

materials so it cannot be used for liquid materials. Furthermore, detection of linear displacement of solid materials based on resonant frequency shifts has been described in [3] where the maximum dynamic range is 12 mm with a sensitivity of 147.8 MHz/mm. Rotation detection of solid materials based on frequency shift has also been described in [19], [21], [23], and [28] where the solid material is moved using a rotator and the sensor is placed on the stator. However, high friction between the material and the sensor has the potential to damage the surface of the resonator and will reduce the performance of the sensor.

Furthermore, a comprehensive comparison of types, sensing parameters and proposed applications of displacement and rotation sensors is shown in Table 3. Previous work [3], [19], [21], [23] proposed a band stop filter for displacement and rotation detection which is recommended for industrial applications including flow detection in liquids, space vehicle and rotation detection in AC motors. In addition, other

work [7], [23], [27], [32] proposed a band stop filter for displacement/rotation detection which is recommended for industrial, biomedical and energy applications while previous work [1], proposed a single port resonator for motor rotation detection AC based on phase variations.

Therefore, this work makes a significant contribution by proposing a dual functional microwave sensor for translation and angular detection in liquid samples using polystyrene-mm pipe channels. The proposed sensor has the capability to detect displacement and angular detection separately based on the frequency shift of the resonator. Polystyrene-mm pipe channels are proposed to reduce the friction between the sensor and the sample and maintain the temperature of the sample in order to obtain high-precision measurements. The proposed sensor has excellent performance with a maximum sensitivity of 31.5 MHz/cm for liquid displacement with a range of $d = 1 - 4$ cm and 0.33 MHz/° for angular detection with an angle range of 0 – 90°.

V. CONCLUSION

A microwave sensor with dual functional characteristics for liquid displacement and angular detection in polystyrene-mm pipe channel has been proposed and presented comprehensively in this paper. The proposed sensor is based on an ELC resonator operating at a resonant frequency of 2.72 GHz. The sample used is liquid material contained in a polystyrene-mm pipe channel. Displacement and angular detection are determined based on the shift in the resonant frequency of the resonator. Based on the measurement results, the proposed sensor has a sensitivity of 31.5 MHz/cm with a displacement range of 1 - 4 cm and 0.33 GHz/° with an angle range of 0 - 90°. This paper makes a significant contribution by proposed a dual functional microwave sensor for displacement and angular detection that can be recommended for the automotive, robotics and aerospace industries.

REFERENCES

- [1] J. Muñoz-Enano, P. Vélez, L. Su, M. Gil-Barba, and F. Martín, "A reflective-mode phase-variation displacement sensor," *IEEE Access*, vol. 8, pp. 189565–189575, 2020, doi: [10.1109/ACCESS.2020.3031032](https://doi.org/10.1109/ACCESS.2020.3031032).
- [2] K. Xu, Y. Liu, S. Chen, P. Zhao, L. Peng, L. Dong, and G. Wang, "Novel microwave sensors based on split ring resonators for measuring permittivity," *IEEE Access*, vol. 6, pp. 26111–26120, 2018, doi: [10.1109/ACCESS.2018.2834726](https://doi.org/10.1109/ACCESS.2018.2834726).
- [3] P.-W. Zhu, X. Wang, W.-S. Zhao, J. Wang, D.-W. Wang, F. Hou, and G. Wang, "Design of H-shaped planar displacement microwave sensors with wide dynamic range," *Sens. Actuators A, Phys.*, vol. 333, Jan. 2022, Art. no. 113311, doi: [10.1016/j.sna.2021.113311](https://doi.org/10.1016/j.sna.2021.113311).
- [4] Z. Shaterian and M. Mrozowski, "Multifunctional bandpass filter/displacement sensor component," *IEEE Access*, vol. 11, pp. 27012–27019, 2023, doi: [10.1109/ACCESS.2023.3258545](https://doi.org/10.1109/ACCESS.2023.3258545).
- [5] J. Naqui and F. Martín, "Angular displacement and velocity sensors based on electric-LC (ELC) loaded microstrip lines," *IEEE Sensors J.*, vol. 14, no. 4, pp. 939–940, Apr. 2014, doi: [10.1109/JSEN.2013.2295518](https://doi.org/10.1109/JSEN.2013.2295518).
- [6] J. Ma, Y. Chen, and J. Huang, "A microwave displacement sensor based on SIW double reentrant cavity with ring gaps," *Prog. Electromagn. Res. M.*, vol. 113, no. 1, pp. 35–45, Sep. 2022, doi: [10.2528/PIERM22050102](https://doi.org/10.2528/PIERM22050102).
- [7] A. V. Praveen Kumar and P. Regalla, "A transmission mode dielectric resonator as a displacement sensor," *IEEE Sensors J.*, vol. 20, no. 13, pp. 6979–6984, Jul. 2020, doi: [10.1109/JSEN.2020.2977893](https://doi.org/10.1109/JSEN.2020.2977893).
- [8] M. Abdolrazzagh, N. Kazemi, V. Nayyeri, and F. Martín, "AI-assisted ultra-high-sensitivity/resolution active-coupled CSRR-based sensor with embedded selectivity," *Sensors*, vol. 23, no. 13, p. 6236, Jul. 2023, doi: [10.3390/s23136236](https://doi.org/10.3390/s23136236).
- [9] M. Abdolrazzagh, N. Katchinskiy, A. Y. Elezabi, P. E. Light, and M. Daneshmand, "Noninvasive glucose sensing in aqueous solutions using an active split-ring resonator," *IEEE Sensors J.*, vol. 21, no. 17, pp. 18742–18755, Sep. 2021, doi: [10.1109/JSEN.2021.3090050](https://doi.org/10.1109/JSEN.2021.3090050).
- [10] N. Kazemi, M. Abdolrazzagh, P. E. Light, and P. Musilek, "In-human testing of a non-invasive continuous low-energy microwave glucose sensor with advanced machine learning capabilities," *Biosensors Bioelectron.*, vol. 241, Dec. 2023, Art. no. 115668, doi: [10.1016/j.bios.2023.115668](https://doi.org/10.1016/j.bios.2023.115668).
- [11] S. Alam, Z. Zakaria, I. Surjati, N. A. Shairi, M. Alaydrus, and T. Firmansyah, "Integrated microwave sensor and antenna sensor based on dual T-shaped resonator structures for contact and noncontact characterization of solid material," *IEEE Sensors J.*, vol. 23, no. 12, pp. 13010–13018, Jun. 2023, doi: [10.1109/JSEN.2023.3273008](https://doi.org/10.1109/JSEN.2023.3273008).
- [12] R. A. Alahnomi, Z. Zakaria, E. Ruslan, S. R. Ab Rashid, and A. A. Mohd Bahar, "High-Q sensor based on symmetrical split ring resonator with spurlines for solids material detection," *IEEE Sensors J.*, vol. 17, no. 9, pp. 2766–2775, May 2017, doi: [10.1109/JSEN.2017.2682266](https://doi.org/10.1109/JSEN.2017.2682266).
- [13] S. Kiani, P. Rezaei, M. Navaei, and M. S. Abrishamian, "Microwave sensor for detection of solid material permittivity in Single/Multilayer samples with high quality factor," *IEEE Sensors J.*, vol. 18, no. 24, pp. 9971–9977, Dec. 2018, doi: [10.1109/JSEN.2018.2873544](https://doi.org/10.1109/JSEN.2018.2873544).
- [14] S. Kiani, P. Rezaei, and M. Navaei, "Dual-sensing and dual-frequency microwave SRR sensor for liquid samples permittivity detection," *Measurement*, vol. 160, Aug. 2020, Art. no. 107805, doi: [10.1016/j.measurement.2020.107805](https://doi.org/10.1016/j.measurement.2020.107805).
- [15] A. A. Abduljabar, H. Hamzah, and A. Porch, "Multi-resonators, microwave microfluidic sensor for liquid characterization," *Microw. Opt. Technol. Lett.*, vol. 63, no. 4, pp. 1042–1047, Apr. 2021, doi: [10.1002/mop.32675](https://doi.org/10.1002/mop.32675).
- [16] M. A. Karimi, M. Arsalan, and A. Shamim, "Multi-channel, microwave-based, compact printed sensor for simultaneous and independent level measurement of eight liquids," *IEEE Sensors J.*, vol. 19, no. 14, pp. 5611–5620, Jul. 2019, doi: [10.1109/JSEN.2019.2904648](https://doi.org/10.1109/JSEN.2019.2904648).
- [17] S. Mosbah, C. Zebiri, D. Sayad, I. Elfergani, M. L. Bouknia, S. Mekki, R. Zegadi, M. Palandoken, J. Rodriguez, and R. A. Abd-Alhameed, "Compact and highly sensitive bended microwave liquid sensor based on a metamaterial complementary split-ring resonator," *Appl. Sci.*, vol. 12, no. 4, p. 2144, Feb. 2022, doi: [10.3390/app12042144](https://doi.org/10.3390/app12042144).
- [18] C.-H. Chio, R. Gómez-García, L. Yang, K.-W. Tam, W.-W. Choi, and S.-K. Ho, "An angular-displacement microwave sensor using an unequal-length-bi-path transversal filtering section," *IEEE Sensors J.*, vol. 20, no. 2, pp. 715–722, Jan. 2020, doi: [10.1109/JSEN.2019.2943640](https://doi.org/10.1109/JSEN.2019.2943640).
- [19] C. H. Chio, R. Gomez-Garcia, L. Yang, K. W. Tam, W.-W. Choi, and S. K. Ho, "An angular displacement sensor based on microwave transversal signal interference principle," *IEEE Sensors J.*, vol. 20, no. 19, pp. 11237–11246, Oct. 2020, doi: [10.1109/JSEN.2020.2998181](https://doi.org/10.1109/JSEN.2020.2998181).
- [20] M. H. Zarifi and M. Daneshmand, "Wide dynamic range microwave planar coupled ring resonator for sensing applications," *Appl. Phys. Lett.*, vol. 108, no. 23, pp. 1–4, 2016, doi: [10.1063/1.4953465](https://doi.org/10.1063/1.4953465).
- [21] A. K. Jha, N. Delmonte, A. Lamecki, M. Mrozowski, and M. Bozzi, "Design of microwave-based angular displacement sensor," *IEEE Microw. Wireless Compon. Lett.*, vol. 29, no. 4, pp. 306–308, Apr. 2019, doi: [10.1109/LMWC.2019.2899490](https://doi.org/10.1109/LMWC.2019.2899490).
- [22] A. Maleki Gargari, B. Ozbey, H. V. Demir, A. Altintas, U. Albostan, and O. Kurc, "A wireless metamaterial-inspired passive rotation sensor with submilliradian resolution," *IEEE Sensors J.*, vol. 18, no. 11, pp. 4482–4490, Jun. 2018, doi: [10.1109/JSEN.2018.2822671](https://doi.org/10.1109/JSEN.2018.2822671).
- [23] J. Naqui and F. Martín, "Transmission lines loaded with bisymmetric resonators and their application to angular displacement and velocity sensors," *IEEE Trans. Microw. Theory Techn.*, vol. 61, no. 12, pp. 4700–4713, Dec. 2013, doi: [10.1109/TMTT.2013.2285356](https://doi.org/10.1109/TMTT.2013.2285356).
- [24] J. Naqui, J. Coromina, A. Karami-Horestani, C. Fumeaux, and F. Martín, "Angular displacement and velocity sensors based on coplanar waveguides (CPWs) loaded with S-shaped split ring resonators (S-SRR)," *Sensors*, vol. 15, no. 5, pp. 9628–9650, Apr. 2015, doi: [10.3390/s150509628](https://doi.org/10.3390/s150509628).
- [25] Z. Mehrjoo, A. Ebrahimi, G. Beziuk, F. Martín, and K. Ghorbani, "Microwave rotation sensor based on reflection phase in transmission lines terminated with lumped resonators," *IEEE Sensors J.*, vol. 23, no. 7, pp. 6571–6580, Apr. 2023, doi: [10.1109/JSEN.2023.3236638](https://doi.org/10.1109/JSEN.2023.3236638).
- [26] J. Muñoz-Enano, P. Vélez, L. Su, M. Gil, P. Casacuberta, and F. Martín, "On the sensitivity of reflective-mode phase-variation sensors based on open-ended stepped-impedance transmission lines: Theoretical analysis and experimental validation," *IEEE Trans. Microw. Theory Techn.*, vol. 69, no. 1, pp. 308–324, Jan. 2021, doi: [10.1109/TMTT.2020.3023728](https://doi.org/10.1109/TMTT.2020.3023728).
- [27] C.-H. Chio, K.-W. Tam, and R. Gómez-García, "Filtering angular displacement sensor based on transversal section with parallel-coupled-line path and U-shaped coupled slotline," *IEEE Sensors J.*, vol. 22, no. 2, pp. 1218–1226, Jan. 2022, doi: [10.1109/JSEN.2021.3133452](https://doi.org/10.1109/JSEN.2021.3133452).
- [28] A. Ebrahimi, W. Withayachumnankul, S. F. Al-Sarawi, and D. Abbott, "Metamaterial-inspired rotation sensor with wide dynamic range," *IEEE Sensors J.*, vol. 14, no. 8, pp. 2609–2614, Aug. 2014, doi: [10.1109/JSEN.2014.2313625](https://doi.org/10.1109/JSEN.2014.2313625).
- [29] J. Mata-Contreras, C. Herrojo, and F. Martín, "Detecting the rotation direction in contactless angular velocity sensors implemented with rotors loaded with multiple chains of resonators," *IEEE Sensors J.*, vol. 18, no. 17, pp. 7055–7065, Sep. 2018, doi: [10.1109/JSEN.2018.2853643](https://doi.org/10.1109/JSEN.2018.2853643).
- [30] G. Keulemans, F. Ceysens, and R. Puers, "An ionic liquid based strain sensor for large displacement measurement," *Biomed. Microdevices*, vol. 19, no. 1, pp. 1–9, 2017, doi: [10.1007/s10544-016-0141-4](https://doi.org/10.1007/s10544-016-0141-4).
- [31] Y. Ren, S. Tan, L. Zhang, Z. Wang, Z. Wang, and J. Yang, "Liquid level sensing using commodity WiFi in a smart home environment," *Proc. ACM Interact., Mobile, Wearable Ubiquitous Technol.*, vol. 4, no. 1, pp. 1–30, Mar. 2020, doi: [10.1145/3380996](https://doi.org/10.1145/3380996).
- [32] M. H. Zarifi, H. Sadabadi, S. H. Hejazi, M. Daneshmand, and A. Sanati-Nezhad, "Noncontact and nonintrusive microwave-microfluidic flow sensor for energy and biomedical engineering," *Sci. Rep.*, vol. 8, no. 1, pp. 1–10, Jan. 2018, doi: [10.1038/s41598-017-18621-2](https://doi.org/10.1038/s41598-017-18621-2).
- [33] A. Ebrahimi, J. Scott, and K. Ghorbani, "Ultrahigh-sensitivity microwave sensor for microfluidic complex permittivity measurement," *IEEE Trans. Microw. Theory Techn.*, vol. 67, no. 10, pp. 4269–4277, Oct. 2019, doi: [10.1109/TMTT.2019.2932737](https://doi.org/10.1109/TMTT.2019.2932737).
- [34] A. A. Abduljabar, H. Hamzah, and A. Porch, "Double microstrip microfluidic sensor for temperature correction of liquid characterization," *IEEE Microw. Wireless Compon. Lett.*, vol. 28, no. 8, pp. 735–737, Aug. 2018, doi: [10.1109/LMWC.2018.2849218](https://doi.org/10.1109/LMWC.2018.2849218).
- [35] S. Alam, Z. Zakaria, I. Surjati, N. A. Shairi, M. Alaydrus, and T. Firmansyah, "Multifunctional of dual-band permittivity sensors with antenna using multicascode T-shaped resonators for simultaneous measurement of solid materials and data transfer capabilities," *Measurement*, vol. 217, Aug. 2023, Art. no. 113078, doi: [10.1016/j.measurement.2023.113078](https://doi.org/10.1016/j.measurement.2023.113078).
- [36] S. Alam, Z. Zakaria, I. Surjati, N. A. Shairi, M. Alaydrus, and T. Firmansyah, "Dual-band independent permittivity sensor using single-port with a pair of U-shaped structures for solid material detection," *IEEE Sensors J.*, vol. 22, no. 16, pp. 16111–16119, Aug. 2022, doi: [10.1109/JSEN.2022.3191345](https://doi.org/10.1109/JSEN.2022.3191345).
- [37] S. Kiani, P. Rezaei, and M. Fakhr, "Real-time measurement of liquid permittivity through label-free meandered microwave sensor," *IETE J. Res.*, pp. 1–11, Jul. 2023, doi: [10.1080/03772063.2023.2231875](https://doi.org/10.1080/03772063.2023.2231875).
- [38] A. Zahedi, F. A. Boroumand, and H. Aliakbarian, "Analytical transmission line model for complex dielectric constant measurement of thin substrates using T-resonator method," *IET Microw., Antennas Propag.*, vol. 14, no. 15, pp. 2027–2034, Dec. 2020, doi: [10.1049/iet-map.2019.1117](https://doi.org/10.1049/iet-map.2019.1117).

- [39] A. A. Abduljabar, N. Clark, J. Lees, and A. Porch, "Dual mode microwave microfluidic sensor for temperature variant liquid characterization," *IEEE Trans. Microw. Theory Techn.*, vol. 65, no. 7, pp. 2572–2582, Jul. 2017, doi: 10.1109/TMTT.2016.2647249.



SYAH ALAM (Graduate Student Member, IEEE) was born in Jakarta, Indonesia. He received the S.Pd. degree in electrical engineering from Universitas Pendidikan Indonesia (UPI), Indonesia, in 2010, the M.Eng. (M.T.) degree in telecommunication engineering from the Graduate Program of Electrical Engineering, Universitas Trisakti, in 2012, and the Ph.D. degree in electronic engineering (RF and microwave) from Universiti Teknikal Melaka Malaysia (UTeM), in 2024.

In 2018, he joined the Department of Electrical Engineering, Universitas Trisakti, as a Researcher and a Lecturer. His research interests include microstrip antenna and microwave sensors for various applications.



INDRA SURJATI (Member, IEEE) was born in Bangkok, Thailand. She received the Bachelor of Engineering (Ir.) degree in electrical engineering and the M.Eng. (M.T.) degree in telecommunication engineering from the Graduate Program of Electrical Engineering, Universitas Trisakti, in 1996, and the Ph.D. degree from the Department of Electrical Engineering, University of Indonesia, in 2004. In 2011, she was a Professor with the Department of Electrical Engineering, Universitas

Trisakti. Her research interests include microstrip antenna and microwave circuits for various applications.



LYDIA SARI (Member, IEEE) received the B.S. degree in electrical engineering from Universitas Trisakti, Jakarta, Indonesia, in 1998, and the M.S. and Ph.D. degrees in electrical engineering from the University of Indonesia in 2002 and 2010, respectively. She is currently a Faculty Member with Electrical Engineering Department, Universitas Trisakti. Her research interests include wireless communications and information theory.



RADEN DEINY MARDIAN (Member, IEEE) received the bachelor's and master's degrees in electrical engineering from Universitas Trisakti, Jakarta, Indonesia, in 1998 and 2001, respectively, and the Ph.D. degree in electrical engineering from Universitas Indonesia, Depok, Indonesia, in 2023. He has published several journal papers and conference proceedings. He is currently a Lecturer at the Electrical Engineering Department, Faculty of Industrial Technology, Universitas Trisakti. His

research interests are mobile and wireless communication technology, digital broadcasting, quality of service, and quality of experience—all his research concerns technical and regulatory policy management.



MAROUANE ABICHA (Student Member, IEEE) was born in Meknes, Morocco. He is currently pursuing the degree in electronics engineering student. His journey in the field of electronics began at the International Academy of Civil Aviation, Casablanca, Morocco, where he pursued his studies, from 2018 to 2020, majoring in electronics and telecommunications. Eager to broaden his horizons, he embarked on a dual-degree program at Polytech Nantes, France, since 2020, specializing

in electronics and digital technologies. During the Summer of 2023, he seized the opportunity to further enrich his academic journey by undertaking an internship at Universitas Trisakti, Jakarta, Indonesia, where he actively contributed to groundbreaking research, specifically delving into the realm of microwave sensors. Currently, in his final year of training, he has honed his expertise in mobile communication systems, with a particular focus on the intricate world of radio frequency environments.



ZAHRIADHA ZAKARIA (Senior Member, IEEE) was born in Johor, Malaysia. He received the B.Eng. and M.Eng. degrees in electrical and electronic engineering from Universiti Teknologi Malaysia, Malaysia, in 1998 and 2004, respectively, and the Ph.D. degree in electrical and electronic engineering from the Institute of Microwaves and Photonics (IMP), University of Leeds, Leeds, U.K., in 2010. From 1998 to 2002, he was with STMicroelectronics, Malaysia, where

he was a Product Engineer. He is currently a Professor with the Microwave Research Group (MRG), Faculty of Electronic and Computer Engineering, Universiti Teknikal Malaysia Melaka (UTeM). He also investigates energy harvesting and sensors. His research interests include a variety of microwave device development, such as planar and nonplanar microwave filters, resonators, amplifiers, and antennas.



TEGUH FIRMANSYAH (Member, IEEE) was born in Subang, Indonesia. He received the B.Eng. and M.Eng. degree in electrical engineering from the Department of Electrical Engineering, Universitas Indonesia, in 2010 and 2012, respectively, and the Dr.Eng. degree (Hons.) from Shizuoka University, Japan, in 2022. In 2012, he joined the Department of Electrical Engineering, Universitas Sultan Ageng Tirtayasa, as a Researcher and a Lecturer. He holds two patents for wideband antenna

and multiband antenna. His research interests include microwave circuits for various applications and developing multifunctional sensors using acoustic, plasmonic, and microwave resonators.



MUDRIK ALAYDRUS (Senior Member, IEEE) was born in Jakarta, Indonesia. He received the Dipl.-Ing. degree in electrical engineering from Universität Hannover, in 1997, and the Dr.-Ing. degree in electrical engineering from the University of Wuppertal, in 2001. Since 2003, he has been with Universitas Mercu Buana, Jakarta. His current research interests include microwave and millimeter wave components, wireless power transfers, wireless sensor networks, an interaction

between electromagnetics and materials, and mathematical modeling in signal processing. He is a member of Verein der Deutschen Elektroingenieure (VDE).



YUSNITA RAHAYU (Senior Member, IEEE) was born in Pekanbaru, Indonesia. She received the B.Eng. degree in electrical engineering from the Department of Electrical Engineering, National Institute of Science and Technology, Jakarta, in 1999, and the M.Eng. and Ph.D. degrees from Universiti Teknologi Malaysia, in 2004 and 2009, respectively. She is currently a Senior Lecturer with the Department of Electrical Engineering, Universitas Riau. Her research interests include

antenna and propagation, microwave and millimeter wave components, sensors, and wireless communication.

...